AD-A276 286
‖‖‖‖‖‖‖‖‖‖‖‖‖‖

AN ADAPTIVE
KALMAN FILTER EXCISOR FOR
SUPPRESSING NARROWBAND INTERFERENCE

by

Brian W. Kozminchuk

94-06299
‖‖‖‖‖‖‖‖‖‖‖‖‖‖

DEFENCE RESEARCH ESTABLISHMENT OTTAWA
TECHNICAL NOTE 93-20

Canada

DTIC QUALITY INSPECTED 1

December 1993
Ottawa

94 2 25 009

Best
Available
Copy

AN ADAPTIVE
KALMAN FILTER EXCISOR FOR
SUPPRESSING NARROWBAND INTERFERENCE

by

Brian W. Kozminchuk
Electronic Support Measures Section
Electronic Warfare Division

DEFENCE RESEARCH ESTABLISHMENT OTTAWA
TECHNICAL NOTE 93-20

ABSTRACT

Several reports have been written by the author which characterize the performance of a Kalman filtering technique to suppress narrowband interference from direct sequence spread spectrum communications systems in a non-adaptive context, i.e., when the user has some *a priori* knowledge of the interference characteristics. This report expands on this technique by presenting an adaptive scheme which is useful for the situation when the interference characteristics are unknown. In this context, the Kalman filter must "learn" to achieve optimal performance through the adjustment of one of its parameters. The criterion for optimality is the minimization of the mean-squared error at the output of the canceller, where this error consists of spread spectrum signal, noise and residual interference. The reasonable assumption is made that minimizing the mean of this squared error with respect to the appropriate Kalman filter parameter is equivalent to minimizing the mean squared value of the residual interference. Examples of the dynamic behaviour of the adaptive interference suppressor are presented for narrowband Gaussian noise interference with bandwidths ranging from 1% to 5% of the chip rate.

RÉSUMÉ

L'auteur de ce rapport a déja publié plusieurs documents sur l'utilisation de filtres de Kalman pour annuler les l'interférences à bandes passantes étroites dans des systèmes de communication utilisant des signaux à spectres étalés par séquences directes. Le cadre de ces travaux était limité à des techniques non adaptatives où les caractéristiques de l'interférence étaient connues, *a priori*, de l'utilisateur. Ce rapport présente des développements où une approche adaptive est utilisée pour annuler des interférences inconnues. Le filtre de Kalman doit alors "apprendre" à ajuster un de ses paramètres pour effectuer le meilleur traitement. L'erreur est constituée du signal à spectre étalé, du bruit et de l'interférence résiduelle, et la minimisation de l'erreur quadratique moyenne à la sortie de l'annuleur sert de critère d'optimisation. On fait l'hypothèse que de minimiser l'erreur quadratique moyenne par rapport au paramètre approprié du filtre de Kalman équivaut à minimiser la valeur quadratique moyenne de l'interférence résiduelle. Des exemples de la dynamique du comportement de l'annuleur adaptatif d'interférence sont présentés pour de l'interférence gaussienne à bande passante étroite (1% à 5% du débit numérique).

EXECUTIVE SUMMARY

This technical note presents an adaptive Kalman filtering technique to suppress narrow-band interference from direct sequence spread spectrum communications systems. This is an expansion of the non-adaptive Kalman filtering approach reported on by the author in earlier reports.

Spread spectrum signals are used extensively in military communication systems. The technique described herein applies equally to both Electronic Support Measures (ESM) systems and direct sequence spread spectrum communication systems. In the former application, the ESM system may be attempting to intercept the spread spectrum signal, but the narrowband interference may be hampering this effort. In the latter application, the spread spectrum communication system may require additional assistance to suppress the interference. Since the open literature has been devoted to this latter case, the material presented here focuses on this application.

One of the attributes of direct sequence spread spectrum communication systems is their ability to combat interference or intentional jamming by virtue of the system's processing gain inherent in the spreading and despreading process. The interference can be attenuated by a factor up to this processing gain. In some cases the gain is insufficient to effectively suppress the interferer, leading to a significant degradation in system performance as manifested by a sudden increase in bit error rate. If the ratio of interference bandwidth to spread spectrum bandwidth is small, the interference can be filtered out to enhance system performance. However, this is at the expense of introducing some distortion onto the signal. This process of filtering is sometimes referred to as interference excision.

The adaptive technique reported upon herein is useful for the situation when the interference characteristics are unknown. In this context, the Kalman filter must "learn" to achieve optimal performance through the adjustment of one of its parameters. The criterion for optimality is the minimization of the mean-squared error at the output of the canceller, where this error consists of spread spectrum signal, noise and residual interference. The reasonable assumption is made that minimizing the mean of this squared error with respect to the appropriate Kalman filter parameter is equivalent to minimizing the mean squared value of the residual interference. Examples of the dynamic behaviour of the adaptive interference suppressor are presented for narrowband Gaussian noise interference with bandwidths ranging from 1 to 5% of the chip rate.

TABLE OF CONTENTS

LIST OF TABLES

LIST OF FIGURES

1.0 INTRODUCTION

Direct sequence spread spectrum communication systems have an inherent processing gain which can reduce the effects of jammers or unintentional interference. When these intruding signals have a power advantage over the spread spectrum system, a severe degradation in communications results. However, communications can be enhanced somewhat by filtering the interference, particularly if its bandwidth is significantly less than the bandwidth of the spread spectrum signal.

Several reports have been written by the author [1, 2, 3, 4, 5] on the performance characteristics of a Kalman filtering approach to narrowband interference suppression in a non-adaptive context, i.e., when the user has some *a priori* knowledge of the interference characteristics. This report focusses on an adaptive scheme which is useful for the situation when these characteristics are unknown, i.e., through some criterion, the Kalman filter must adjust its parameters to achieve optimal performance.

The outline of the report is as follows. Sections 2.0 and 3.0 review the basic elements of the non-adaptive interference suppression system, with Section 2.0 describing the spread spectrum communications model and Section 3.0 detailing the interference estimator. This latter section includes: a description of the state space model which generates a function related to the interference; the extended Kalman filter algorithm and resultant digital phase-locked loop (DPLL) which is used to estimate the interferer's phase; and the envelope estimator which is combined with the output of the Kalman filter to produce an estimate of the interference. Section 4.0 describes the adaptive algorithm which is based on minimizing the mean-squared value of the error signal at the output of the canceller while one of the Kalman filter parameters is adjusted over time in a controlled fashion. This section also includes simulation results for the case of narrowband Gaussian noise of different bandwidths corrupting the spread spectrum signal. Finally, Section 5.0 summarizes the results of this report and suggests areas for further research.

2.0 COMMUNICATIONS MODEL

The basic elements of the BPSK PN spread spectrum system are shown in Fig. 1. The received waveform $r(t)$, consisting of a spread spectrum signal, additive white Gaussian noise, and narrowband interference is applied to a bandpass filter with the transfer function $H_{bp}(f)$, whose output is defined as

$$u(t) = s(t) + n(t) + i(t). \tag{1}$$
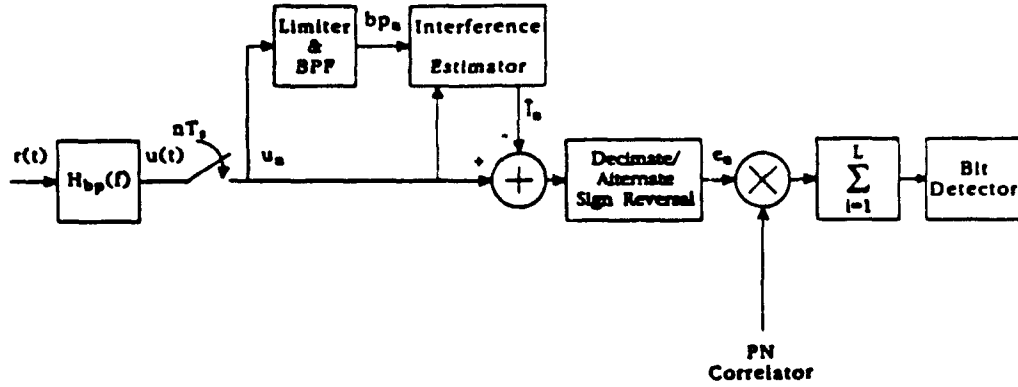
Figure 1: Spread spectrum communications model.

The bandpass filter $H_{bp}(f)$, for the application considered here, is assumed to be a filter matched to a chip and centered at the carrier frequency ω_0 of the spread spectrum signal defined as

$$s(t) = a(t)\cos(\omega_0 t) \tag{2}$$

where

$$a(t) = \sum_k D_k b_k(t - kT_b). \tag{3}$$

In Eq. (3), D_k is a sequence of data bits of amplitude (± 1), T_b is the reciprocal of the bit rate R_b, and $b_k(t - kT_b)$ is the PN sequence pattern for the kth bit, i.e.,

$$b_k(t) = \sum_{j=1}^{L} c_{kj} q(t - jT_c) \tag{4}$$

with L being the number of pseudo random chips per bit, or the processing gain, c_{kj} is the code sequence for the bit, T_c is the recipro $:$al of the chip rate R_c and $q(t)$ represents the basic chip pulse of energy E_c.

The noise $n(t)$ in Eq. (1) is Gaussian and has a power spectral density

$$S_n(f) = \frac{N_0}{2}|H_{bp}(f)|^2, \tag{5}$$

where $N_0/2$ is the power spectral density of the assumed white Gaussian noise from the channel. The interference term in Eq. (1) is of bandwidth $B_i << 2R_c$ and is defined as

$$i(t) = I(t)\cos(\omega_0 t + \theta(t)) \tag{6}$$

2

where $I(t)$ is the interference amplitude and $\theta(t)$ is the phase modulation. It has been assumed that the effect of the bandpass filter $H_{bp}(f)$ is negligible on the interference $i(t)$.

Referring to Fig. 1, the output $u(t)$ of the bandpass filter $H_{bp}(f)$ of gain $\sqrt{E_cT}$ is bandpass sampled and applied to a limiter/bandpass filter and interference estimator.

Consider the bandpass sampler first. The analog signal $u(t)$ from Eq. (1) is sampled at $f_s = 2R_c$ ($mf_s = \omega_0/2\pi + R_c/2$ for some integer m). The resultant sampled signal is, therefore,

$$u_n = s_n + n_n + i_n. \tag{7}$$

where s_n consists of the sequence $\{\ldots, 0, (-1)^n a_n, 0, (-1)^{n+2} a_{n+2}, \ldots\}$ where the a_n are of energy E_c and coded according to $c_{k_j} D_k$ for the jth chip in the kth transmitted bit, n_n [1] are uncorrelated Gaussian noise samples of variance $\sigma_{nse}^2 = E_c(N_0/2)$, and i_n is the sampled version of Eq. (6). The samples u_n are applied to the interference estimator and interference canceller.

Consider now the branch containing the limiter. Here, u_n is applied to a limiter/bandpass filter. The input to the limiter referenced to the interference is redefined as

$$u_n = \sqrt{[i_n + n'_{1,n} + a'_{1,n}]^2 + [n'_{2,n} + a'_{2,n}]^2}\, \cos[\omega_0 n + \theta_n + \phi_{u,n}] \tag{8}$$

where

$$\phi_{u,n} = \arctan\left(\frac{n'_{2,n}/\sqrt{2} + a'_{2,n}}{I_n + n'_{1,n}/\sqrt{2} + a'_{1,n}}\right) \tag{9}$$

is a noise-like phase fluctuation on the interferer's phase θ_n, and is due to the noise and spread spectrum signal. The terms $n'_{1,n}$, $n'_{2,n}$, $a'_{1,n}$ and $a'_{2,n}$ are in-phase and quadrature components of the noise and spread spectrum signal with respect to the interference phase θ_n. The output of the limiter/bandpass filter is [6]

$$bp_n = \frac{4A'}{\pi}\cos[\omega_0 n + \theta_n + \phi_{u,n}], \tag{10}$$

where A' is the limiter's output level. This signal is redefined as (letting $A' = \sqrt{2}\pi/4$ for convenience)

$$bp_n = \sqrt{2}\cos[\omega_0 n + \theta_n + \phi_{u,n}]. \tag{11}$$

It should be noted that for large interference-to-noise ratios in which the interference is of constant envelope, $\phi_{u,n}$ in Eq. (11) is approximately Gaussian [6]. The sampled signal

---

[1] Coherent bandpass sampling has been assumed, so that the in-phase component is $(n_{1,n}/\sqrt{2})\cos(n\pi/2)$ and the quadrature component is $(n_{2,n}/\sqrt{2})\sin(n\pi/2)$

in Eq. (11) is what is processed by the Kalman filter, which estimates the phase θ_n of the interference.

3.0 THE INTERFERENCE ESTIMATOR

This section presents the interference estimator. It consists of the extended Kalman filter which estimates the phase of the interference, and the envelope estimator which is combined with the Kalman filter result to produce an estimate of the interference.

First, the analog and digital state space models on which the Kalman filter algorithm is based will be presented. This will be followed by the extended Kalman algorithm used to estimate the state variables. Finally, the section concludes with two structures for estimating the interference using the results of the Kalman filter and envelope estimator.

3.1 THE STATE SPACE MODEL

The development here follows that in [7]. A block diagram of the analog state space model which generates the analog version of a function related to bp_n in Eq. (11) is shown in Fig. 2; this function is represented by $bp(t)'$ [2] which is defined later in this section. The state space equations are defined as

$$\begin{bmatrix} \dot{x}_1(t) \\ \dot{x}_2(t) \end{bmatrix} = \begin{bmatrix} 0 & d \\ 0 & -\alpha \end{bmatrix} \begin{bmatrix} x_1(t) \\ x_2(t) \end{bmatrix} + \begin{bmatrix} 0 \\ \sqrt{K_w} \end{bmatrix} w(t), \tag{12}$$

where $x_1(t)$ and $x_2(t)$ are the phase function and modulating signal state variables of the interference, respectively. In compact form Eq. (12) becomes

$$\dot{x}(t) = Ax(t) + gw(t). \tag{13}$$

The interferer's modulating signal $x_2(t)$ is assumed to be generated by applying Gaussian white noise, $w(t)$, of unit variance to an amplifier with gain $\sqrt{K_w}$ followed by a first order low pass filter of bandwidth $\alpha = 2\pi\alpha_f$. The steady state variance of the coloured noise at the output of the lowpass filter is unity if $K_w = 2\alpha$. The output is multiplied by the frequency deviation constant, d, and then integrated to yield the phase function

$$x_1(t) = d \int_0^t x_2(\tau)\, d\tau. \tag{14}$$

---

[2] In the analog version of Eq. (11), the noise is one of the arguments of the cosine function. For the model discussed here, the noise will be additive.

4

An FM type of signal (interferer) is generated by phase modulating a carrier, ω_0, which has been set equal to the carrier of the spread spectrum signal, since any offsets from ω_0 can be incorporated into $x_1(t)$, yielding

$$y(t) = \sqrt{2}\cos[\omega_0 t + x_1(t)]. \tag{15}$$

This signal is corrupted by white Gaussian noise $v(t)$ with power spectral density $N_{obs}/2$ generally different from $N_0/2$ defined earlier for the communications model in Fig. 1. The result is an FM signal related to the interference in Eq. (11) except for the fact that the noise term is additive here, i.e.,

$$bp'(t) = y(t) + v(t). \tag{16}$$

For large interference-to-signal-plus-noise conditions, the final effect of the additive noise in estimating the phase $x_1(t)$ in Eq. (15) will be similar to the effect of $\phi_{u,n}$ in Eq. (11).

Given the observation process $bp'(t)$ from Eq. (16), the objective is to estimate the state $x_1(t)$ and the related state $x_2(t)$, as well as $y(t)$ in Eq. (15). One approximate technique reserved for nonlinear estimation problems [8] is the extended Kalman filter algorithm.
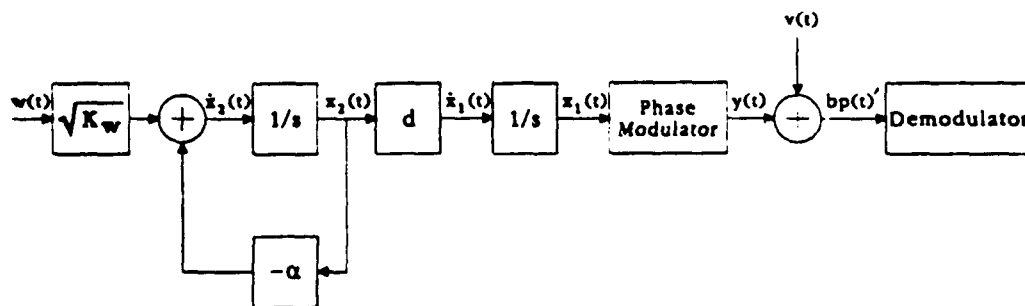


Figure 2: Block diagram of the state space model.

Before the algorithm is presented, the discrete forms of Eqs. (12) and (13) will be stated, namely,

$$x_{n+1} = \phi x_n + w_n. \tag{17}$$

where n represents discrete time,

$$\phi = \begin{bmatrix} 1 & \beta(1 - e^{-\alpha T_s}) \\ 0 & e^{-\alpha T_s} \end{bmatrix} = \begin{bmatrix} 1 & \phi_{12} \\ 0 & \phi_{22} \end{bmatrix} \tag{18}$$

and

$$w_n = \int_{nT_s}^{(n+1)T_s} \phi g\, w(z)\, dz. \tag{19}$$

In Eq. (18), $\beta = d/\alpha$ and is termed the bandwidth expansion ratio in units of $volts^{-1}$ [9]. In Eq. (19), w_n is a stationary zero-mean white Gaussian vector sequence whose covariance, (i.e., $E\{w_n w_n^t\}$), is given by

$$V_w = \int_{nT_s}^{(n+1)T_s} \phi g g^t \phi\, du. \tag{20}$$

Finally, Eq. (16) becomes,

$$bp_n' = y_n + v_n, \tag{21}$$

where y_n is the sampled version of Eq. (15), i.e.,

$$y_n = \sqrt{2}\cos(\omega_0 n + x_{1,n}) \tag{22}$$

It has been assumed that $bp'(t)$ from Eq. (16) has been applied to a bandpass filter of bandwidth B, whose output has been sampled at a rate so as to yield uncorrelated noise samples v_n of variance $\sigma_v^2 = B(N_{obs}/2)$ [10].

The noise covariance matrix, V_w, is obtained by substituting Eq. (18) and g from Eq. (13) into Eq. (20) and integrating each term, yielding

$$V_w = \frac{K_w}{2\alpha} \left[\begin{array}{cc} \beta^2\left(4\pi/\gamma - 3 + 4e^{-2\pi/\gamma} - e^{-4\pi/\gamma}\right) & \beta\left(1 - e^{-2\pi/\gamma}\right) \\ \beta\left(1 - e^{-2\pi/\gamma}\right) & 1 - e^{-4\pi/\gamma} \end{array} \right] \tag{23}$$

where $\gamma = 2\pi/(\alpha T_s)$, which is the ratio of the sampling rate $f_s = 1/T_s$ to the interferer's modulating signal bandwidth α_f. The discrete form of the interference model is shown in Fig. 3.

3.2 EXTENDED KALMAN FILTER EQUATIONS

The extended Kalman filter equations [8] can now be applied to the discrete model. The resulting algorithm is listed in Table 1. In the algorithm $\hat{x}_n$ is defined as the estimate of the true state vector x_n, $\tilde{x}_n$ is defined as the post error $x_n - \hat{x}_n$, K_n is the Kalman gain vector, $V_{\tilde{x}_n} = E\{\tilde{x}_n \tilde{x}_n^t\}$ is the post error covariance and $V_{\tilde{x}_{n|n-1}} = E\{\tilde{x}_{n|n-1}\tilde{x}_{n|n-1}^t\}$ is the prior error covariance. Furthermore, $f_{n|n-1}^{-1}$ is known as the "coupled equation", since the estimate of the interferer's phase is contained in it. However, this equation can be

6
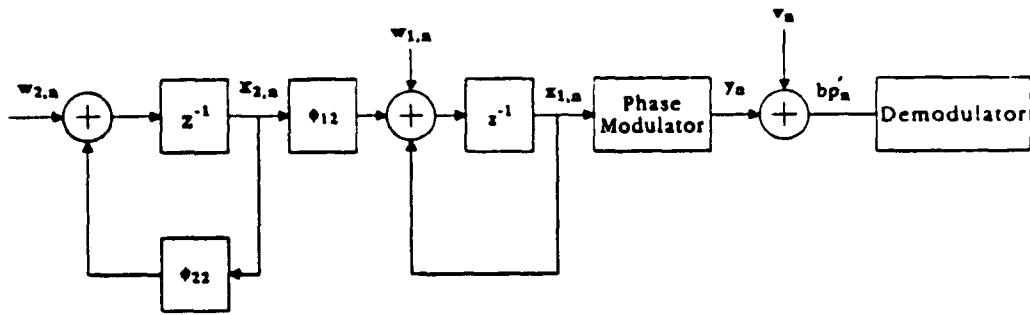
Figure 3: Discrete form of the interference model.

further approximated as noted in [7]. The approximation is

$$f_{n|n-1}^{-1} \approx \frac{1}{V_{\hat{x}_{11,n|n-1}}} \left\{ 1 - \sqrt{\frac{\sigma_v^2}{\sigma_v^2 + V_{\hat{x}_{11,n|n-1}}}} \right\}. \tag{24}$$

3.3 THE DIGITAL PHASE-LOCKED LOOP (DPLL)

The Kalman algorithm results in a digital PLL [7]. This fact will be elaborated upon here so as to illustrate the sampling rate requirements which are related to the allowable interference bandwidths which the system is capable of handling.

Substitution of the Kalman gain K_n from Table (1) into the state estimate equation for $\hat{x}_n$ yields

$$\hat{x}_n = \phi \hat{x}_{n-1} + V_{\hat{x}_n} \begin{bmatrix} 1/\sigma_v^2 \\ 0 \end{bmatrix} \left\{ -bp_n' \sqrt{2} \sin[\omega_0 n + \hat{\theta}_{n|n-1}] \right.$$
$$+ \left. \sin[\omega_0 n + \hat{\theta}_{n|n-1}] \cos[\omega_0 n + \hat{\theta}_{n|n-1}] \right\} \tag{25}$$

Consider the term within braces. Substituting for bp_n' from Eq. (21) and noting that $x_{1,n} = \theta_n$, one obtains the intermediate variable

$$h_n = \sin(\theta_n - \hat{\theta}_{n|n-1}) - \sin(2\omega_0 n + \theta_n + \hat{\theta}_{n|n-1})$$
$$+ \sin(2\omega_0 n + 2\theta_n) - \sqrt{2} v_n \sin(\omega_0 n + \hat{\theta}_{n|n-1}) \tag{26}$$

which consists of four terms. The first refers to the baseband term. The second and third are second harmonic terms. Recalling that v_n is the sampled version of bandpass noise centered at ω_0, the fourth term turns out to be baseband noise which can be modeled as

7

Table 1: The Kalman Filter Algorithm.

<u>Initial Conditions:</u>

$$\hat{x}_{-1} = E\{\hat{x}_{-1}\} = \begin{bmatrix} m_1 \\ m_2 \end{bmatrix}; \quad V_{\tilde{x}_{-1}} = E\{\tilde{x}_{-1}\tilde{x}_{-1}^t\}$$

<u>Do for $n = 0$ to T:</u>

$$\hat{\theta}_{n|n-1} = \begin{bmatrix} 1 & 0 \end{bmatrix} \phi \hat{x}_{n-1}$$

$$V_{\tilde{x}_{n|n-1}} = \phi V_{\tilde{x}_{n-1}} \phi^t + V_w$$

$$f_{n|n-1}^{-1} = \frac{1 - \cos(2\omega_0 n + 2\hat{\theta}_{n|n-1})}{\sigma_v^2 + V_{\tilde{x}_{11,n|n-1}} \left[1 - \cos(2\omega_0 n + 2\hat{\theta}_{n|n-1})\right]}$$

$$V_{\tilde{x}_n} = V_{\tilde{x}_{n|n-1}} - V_{\tilde{x}_{n|n-1}} \begin{bmatrix} 1 & 0 \\ 0 & 0 \end{bmatrix} V_{\tilde{x}_{n|n-1}} f_{n|n-1}^{-1}$$

$$K_n = -V_{\tilde{x}_n} \begin{bmatrix} 1/\sigma_v^2 \\ 0 \end{bmatrix} \sqrt{2} \sin(\omega_0 n + \hat{\theta}_{n|n-1})$$

$$\hat{x}_n = \phi \hat{x}_{n-1} + K_n \left[b\dot{p}_n' - \sqrt{2}\cos(\omega_0 n + \hat{\theta}_{n|n-1})\right]$$

a zero mean white Gaussian noise process [9]. The first and fourth terms are the desired ones, since they correspond to their analog PLL counterparts. Also, as in the analog implementation, the second harmonic terms can be neglected, provided they do not alias into the baseband region.

To ensure that no spectral aliasing of these terms occurs, the sampling rate must be selected according to $f_s \geq 4B_i$. This can be seen from the following heuristic argument. As a starting point consider analog spectra. Then assume that no noise is present and $\hat{\theta}(t) \approx \theta(t)$. Also let the terms within braces in Eq. (25) be represented as follows:

$$q_1(t) = bp'(t) = \sqrt{2}\cos[\omega_0 t + \theta(t)] \qquad (27)$$

$$q_2(t) = \sqrt{2}\sin[\omega_0 t + \hat{\theta}(t)] \qquad (28)$$

$$\begin{aligned} q_3(t) &= \sin[\omega_0 t + \hat{\theta}(t)]\cos[\omega_0 t + \hat{\theta}(t)] \\ &= \frac{1}{2}\sin[2\omega_0 t + 2\hat{\theta}(t)]. \end{aligned} \qquad (29)$$

The amplitude spectrum of $q_1(t)$ is shown in Fig. 4(a). It is assumed that the amplitude spectrum of $q_2(t)$ is approximately equal to it for the case of $\theta(t) \approx \hat{\theta}(t)$. Taking the product of $q_1(t)$ and $q_2(t)$ in Eqs. (27) and (28) results in

$$q_4(t) = \sin[\theta(t) - \hat{\theta}(t)] + \sin[2\omega_0 t + \theta(t) + \hat{\theta}(t)] \qquad (30)$$

whose spectrum is shown in Fig. 4(b), the convolution of $Q_1(f)$ and $Q_2(f)$. If an integer multiple of the sampling frequency mf_s is chosen as shown in Fig. 4(b) then the required sampling rate for no aliasing in the baseband region is $f_s \geq 4B_i$. Thus, the baseband and second harmonic terms interleave as shown in Fig. 4(c). Similarly, the spectrum for $q_3(t)$ and its sampled spectrum are shown in Figs. 5(a) and (b).

The second harmonic terms can therefore be neglected and Eq. (25) becomes

$$\begin{aligned} \hat{x}_n &= \phi\hat{x}_{n-1} + V_{\tilde{x},n}\begin{bmatrix} 1/\sigma_v^2 \\ 0 \end{bmatrix}\left\{-bp'_n\sqrt{2}\sin[\omega_0 n + \hat{\theta}_{n|n-1}]\right\} \\ &= \phi\hat{x}_{n-1} + V_{\tilde{x},n}\begin{bmatrix} 1/\sigma_v^2 \\ 0 \end{bmatrix}\left\{\sin[\theta - \hat{\theta}_{n|n-1} + v'_n]\right\} \end{aligned} \qquad (31)$$

where

$$v'_n = -\sqrt{2}v_n\sin[\omega_0 n + \hat{\theta}_{n|n-1}] \qquad (32)$$

9
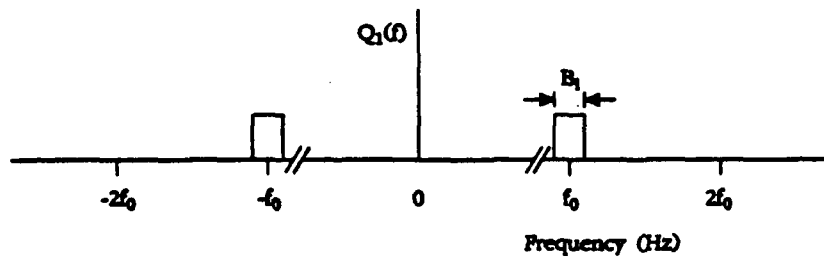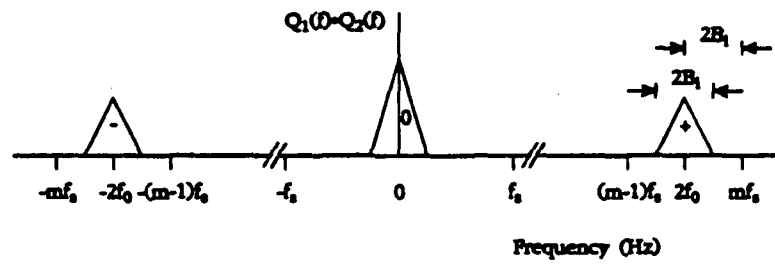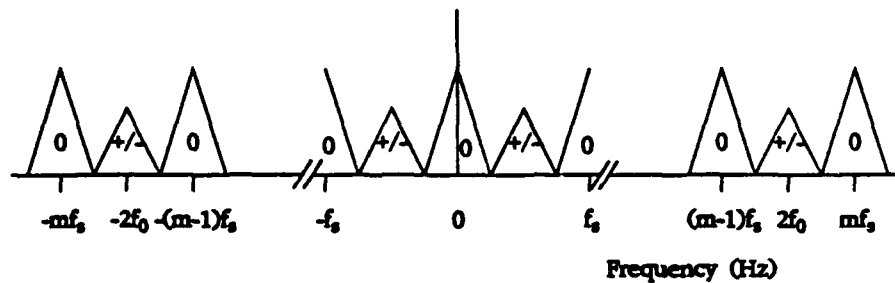
Figure 4: Illustration of the sampling rate requirements: (a) Hypothetical interference spectrum of $q_1(t)$; (b) Convolution of $Q_1(f)$ with $Q_2(f)$; (c) Sampled spectrum of the product $q_1(t)q_2(t)$.

10
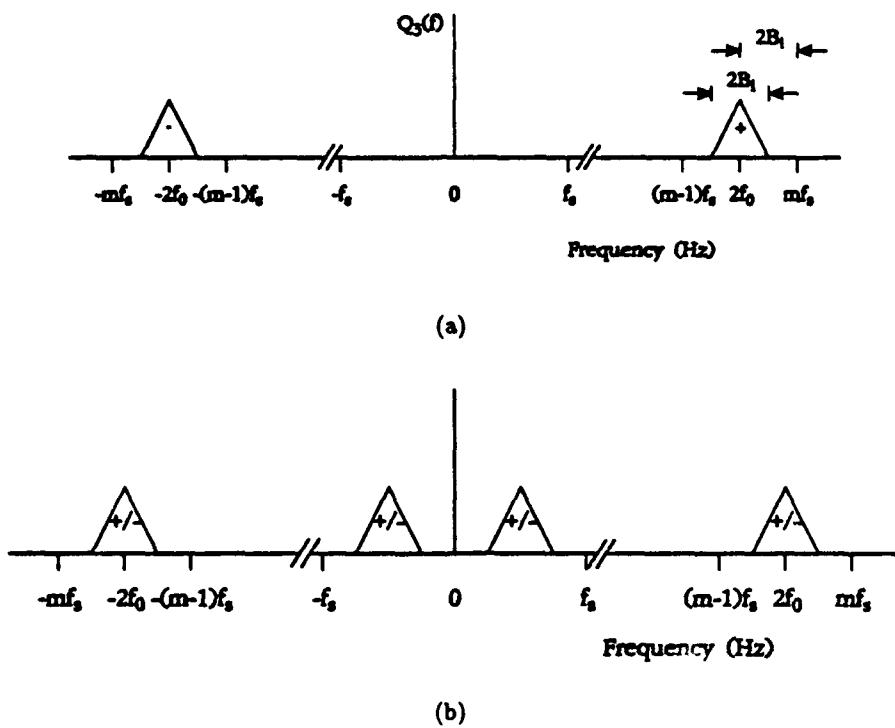
Figure 5: Analog and sampled spectra of $q_3(t)$ (see Eq. (29)).

and is of variance $(N_{ob_s}/2)f_s$.

The state space diagram of the DPLL is illustrated in Fig. 6. Observe that
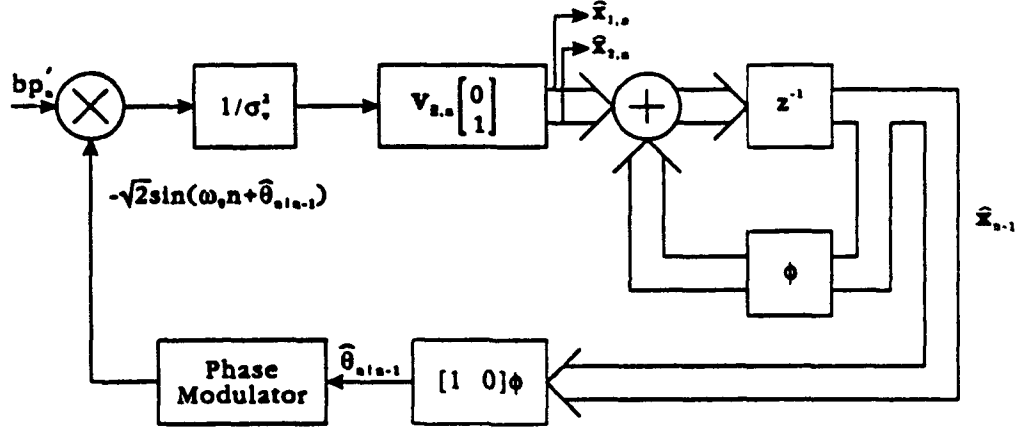
Figure 6: State space representation of the DPLL.

the phase estimate $\hat{\theta}_{n|n-1}$ is applied to a phase modulator of frequency ω_0, resulting in a "VCO" signal defined as

$$VCO_n = -\sqrt{2}\sin(\omega_0 n + \hat{\theta}_{n|n-1}). \tag{33}$$

Shifting this signal by $-\pi/2$ radians results in a filtered estimate of y_n in Eq. (21).

It should be noted that the Kalman algorithm in Table (1) which is based on the state space model shown in Fig. 2 will lead to a steady state error if the phase θ_n is a ramp. The steady state error can be reduced to zero by modifying the interference model [11]. The modification involves replacing the low pass filter in Fig. 2 by an integrator (i.e., by setting $\alpha = 0$ in A in Eq. (13)). With this change, the state transition matrix ϕ and covariance matrix V_w become, respectively,

$$\phi = \begin{bmatrix} 1 & dT_s \\ 0 & 1 \end{bmatrix} = \begin{bmatrix} 1 & \phi_{12} \\ 0 & \phi_{22} \end{bmatrix} \tag{34}$$

and

$$V_w = \frac{K_w}{2\alpha} \begin{bmatrix} 2\beta^2\alpha^3 T_s^3 & 2\beta\alpha^2 T_s^2 \\ 2\beta\alpha^2 T_s^2 & 2\alpha T_s \end{bmatrix}. \tag{35}$$

Using these terms in the Kalman equations results in a slightly modified algorithm. This is the algorithm that has been used in the simulations.

12

3.4 INTERFERENCE ESTIMATOR STRUCTURES

This section presents two structures for the interference estimator shown in Fig. 1 and which includes the Kalman filter discussed in the previous section. These structures have been used in connection with the non-adaptive Kalman algorithm [5, 12] and are presented here for later reference.

As noted earlier, the Kalman algorithm produces a filtered estimate of y_n in Eq. (22), which can be used as a basis for estimating a sampled version of the envelope of $i(t)$ (i.e., I_n in Eq. (6)) which is mixed with the same y_n to yield an estimate of the interference. The first structure is a straightforward implementation of this idea. The second structure carries out additional phase-smoothing on the Kalman filter phase estimate; this adds extra complexity, but improves the performance somewhat [12].

The first structure is illustrated in Fig. 7. The output of the first multiplier is a baseband term and is, using Eq. (7), excluding the $\sqrt{2}$ factor,

$$
\begin{aligned}
\hat{I}'_n \ = \ & I_n \cos(\theta_n - \hat{\theta}_{n|n-1}) \\
& + \ n_n \cos(\omega_0 n + \hat{\theta}_{n|n-1}) + a_n \cos(\hat{\theta}_{n|n-1}) \\
& + \ a_n \cos(2\omega_0 n + \hat{\theta}_{n|n-1}).
\end{aligned}
\tag{36}
$$

Equation (36) consists of four terms: the first term is related to the desired amplitude of
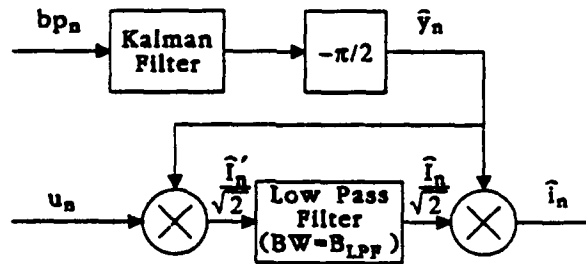
Figure 7: Block diagram of the interference estimator.

the interference; the second is approximately Gaussian baseband noise [9]; and the third and fourth terms are noise-like terms emanating from the spread spectrum signal. The fourth term, because of the sampling rate conditions discussed in Section 3.3, is essentially filtered out by the low pass filter of bandwidth $B_{LPF} < 0.50$ Hz and, therefore, will be ignored in the baseband simulations to be discussed in the next chapter. The term $\hat{I}'_n/\sqrt{2}$ is filtered, resulting in the estimate of the interference envelope, $\hat{I}_n/\sqrt{2}$. Combining this

with an estir. te of y_n in Eq. (22), $\hat{y}_n$, shown in Fig. 7 yields the estimate of the interference

$$\hat{\imath}_n = \hat{I}_n \cos(\omega_0 n + \hat{\theta}_{n|n-1}), \tag{37}$$

which is subtracted from u_n as illustrated in Fig. 1. Because the input was coherently bandpass sampled at twice the chip rate, the output of the canceller (summer) undergoes decimation and alternate sign reversal, resulting in the error signal e_n, which undergoes correlation with the local PN code and bit detection.

The second structure is illustrated in Fig. 8. There were two reasons for introducing this structure. The first was to counter the effects of the group delay produced by the Butterworth low pass filter in Fig. 7 by using a linear phase FIR filter with known delay D. The second was to do some additional smoothing on the phase estimate $\hat{\theta}_{n|n-1}$ from the Kalman filter which would introduce the same delay D. With phase-smoothing and the FIR low pass filter, the interference estimate becomes $\hat{\imath}_{n-D}$ which is subtracted from a delayed version of the input, u_{n-D}. The result is the error signal e_{n-D} which is applied to the PN correlator whose PN sequence is delayed by D samples as well.
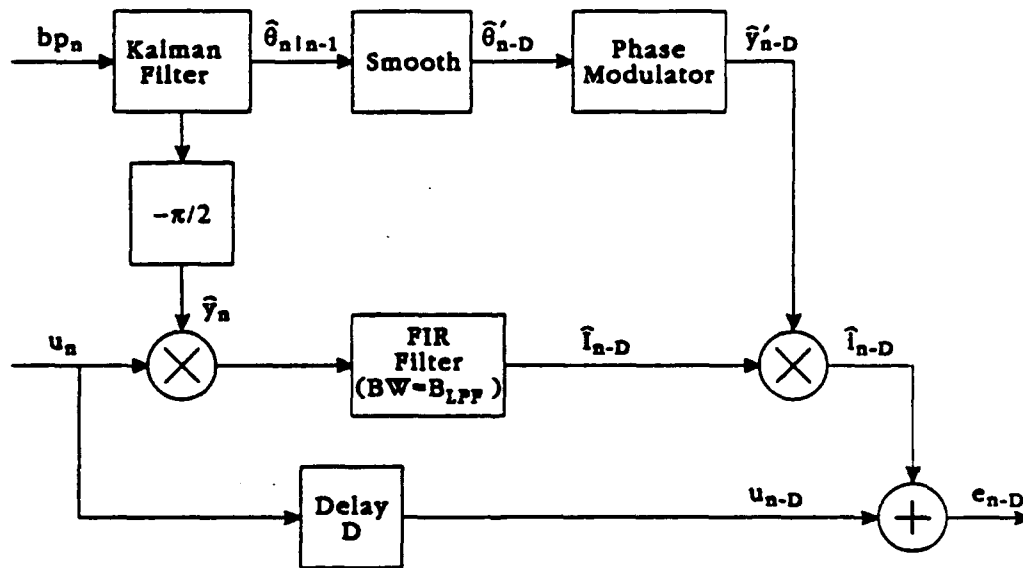

Figure 8: Interference estimator when phase-smoothing is being used.

14

4.0   AN ADAPTIVE KALMAN FILTER EXCISOR

To this point, a non-adaptive Kalman filter has been presented. It will be shown that by varying the frequency deviation constant d, while keeping the variance σ_v^2 of the observation noise and the modulating signal bandwidth α_f of the Kalman filter model for FM interference fixed, a minimum for the mean-squared value of the residual interference, $E\{\Delta i^2\}$, can be obtained. This suggests an adaptive scheme which this section is concerned with.

The proposed scheme is to vary d over time (with σ_v^2 and α_f fixed) and to monitor an estimate of $E\{e_n^2\}$, the mean-squared value of the excisor's error signal in Fig. 1, which is related to $E\{\Delta i^2\}$ as discussed below.
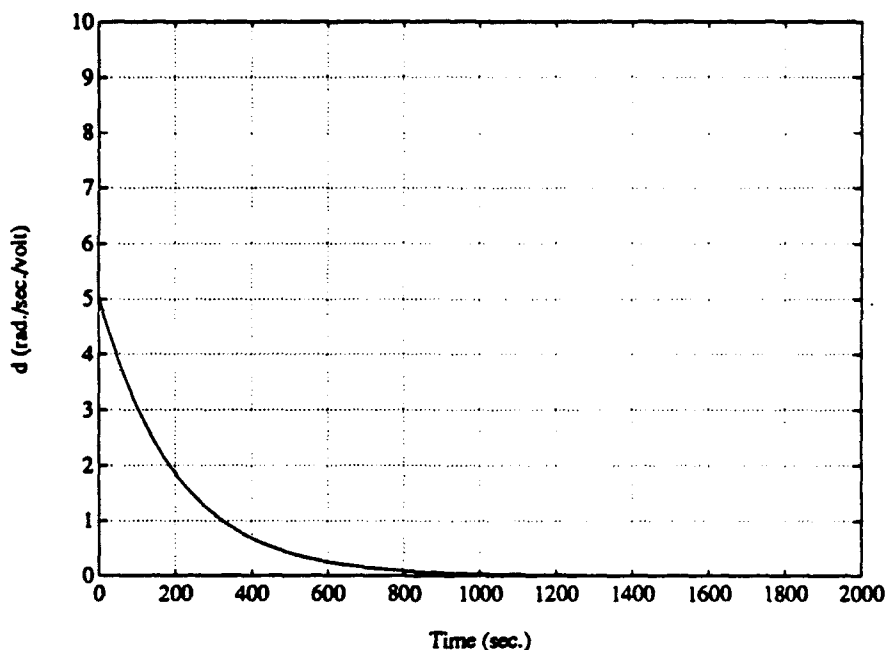

Figure 9: Profile of the frequency deviation constant d used in the phase- and envelope-tracking tests.

As an example, Fig. 9 illustrates a time-varying frequency deviation constant d. The interference for this case was narrowband Gaussian noise with bandwidth $B_i = 0.01$ Hz and the interference estimator was the system in Fig. 7 with $B_{LPF} = 0.40$ Hz. The phase- and envelope-tracking capabilities of a combination of the Kalman filter and envelope estimator arising from this time-varying function are shown in Figs. 10 and 11.

15

Referring to Fig. 10, for large values of d, the phase-noise is evident until at about 400 iterations, at which point the phase-noise has decreased substantially, indicating that the bandwidth of the Kalman filter has decreased. Observe also that initially, the algorithm exhibits some slippage, taking from 10 to 15 radians before it settles down to a tracking error of 2π radians after approximately 50 iterations; the slippage is, in part, due to d being initially too large. At the other extreme, when d becomes too small, the algorithm eventually loses track because the rate of change of the phase is too fast for it (i.e., the bandwidth of the Kalman filter is too small).
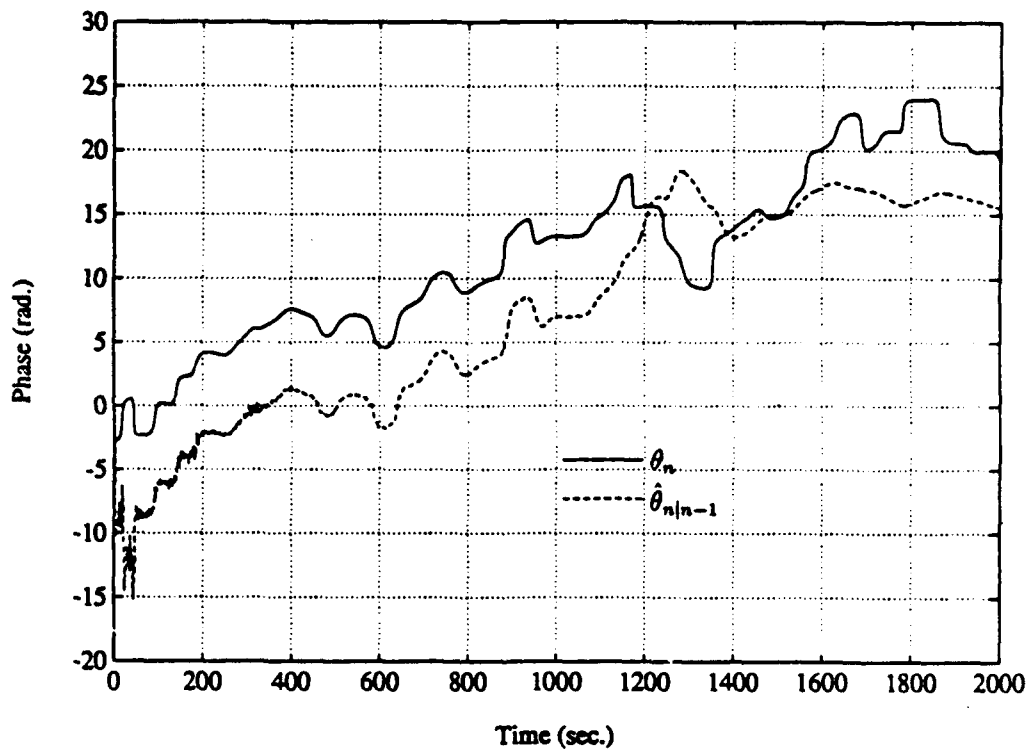

Figure 10: An example of the phase-tracking capability of the Kalman filter when the frequency deviation constant d was varied according to the profile in Fig. 9.

Figure 11 illustrates the estimate of the envelope of the interference during the same time period. As d decreases, $\dot{i}_n$ appears to improve, until at approximately 1200 iterations, the estimate degrades substantially due to the inability of the Kalman filter to adequately track the phase θ_n as shown in Fig. 10.
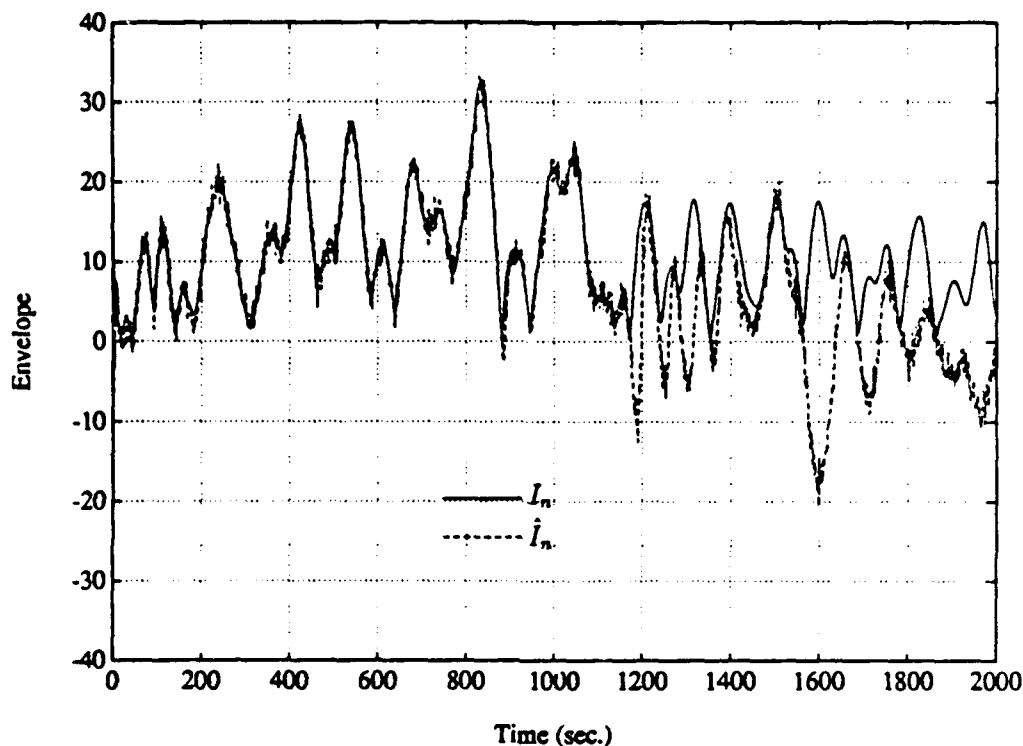

Figure 11: An example of the envelope-tracking capability of the Kalman filter when the frequency deviation constant d was varied according to the profile in Fig. 9.

The results in Figs. 10 and 11 suggest that an optimum value of d exists that will lead to accurate tracking of the interferer and minimum mean-squared interference error; it also suggests a strategy for an adaptive algorithm. An architecture that illustrates the concept is shown in Fig. 12, which is based on finding that value of d which minimizes the mean-squared value of e_n at the input to the PN correlator. This concept is based on the use of the interference estimator in Fig. 7. Figure 12 would have to be modified appropriately by incorporating a delay of D samples in u_n and the PN correlator if Fig. 8 would be used; the results presented later in this section are based on this latter approach.
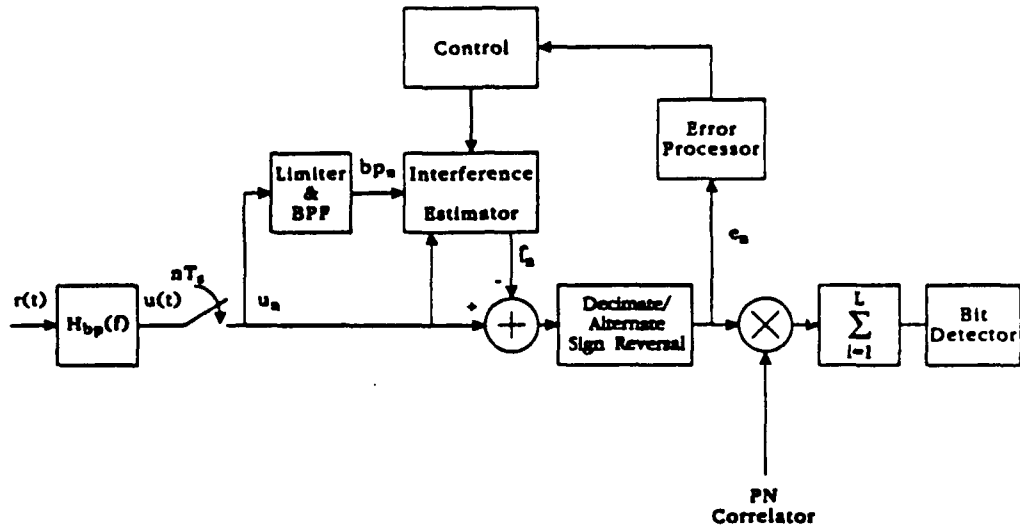
Figure 12: Adaptive architecture, which is based on minimizing the squared error of the error signal e_n, while varying d.

Minimizing the mean-squared value of e_n is equivalent to determining the minimum of

$$
\begin{aligned}
E\{e_n^2\} &= E\{(s_n + n_n + \Delta i)^2\} \\
&\approx E\{s_n^2\} + E\{n_n^2\} + E\{\Delta i^2\}
\end{aligned}
\tag{38}
$$

where Δi^2 is the residual interference which has been defined in [5]. The assumptions which were made so that the terms in Eq. (38) could be de-coupled are also contained in [5].

Figure 13 conceptually shows the steps of the adaptive process. Figure 13(a) illustrates an example of the d profile which is decreased according to the equation

$$
d_n = d_0 \exp^{-c_0 n},
\tag{39}
$$

where d_0 is the initial condition, and c_0 controls the rate of change of d_n. This part of the profile forms the search phase, during which time an estimate of the mean-squared value of the error e_n at the input to the PN correlator is continually being calculated using the relation

$$
\overline{e_n^2} = \xi_1 \overline{e_{n-1}^2} + (1 - \xi_1) e_n^2
\tag{40}
$$

18
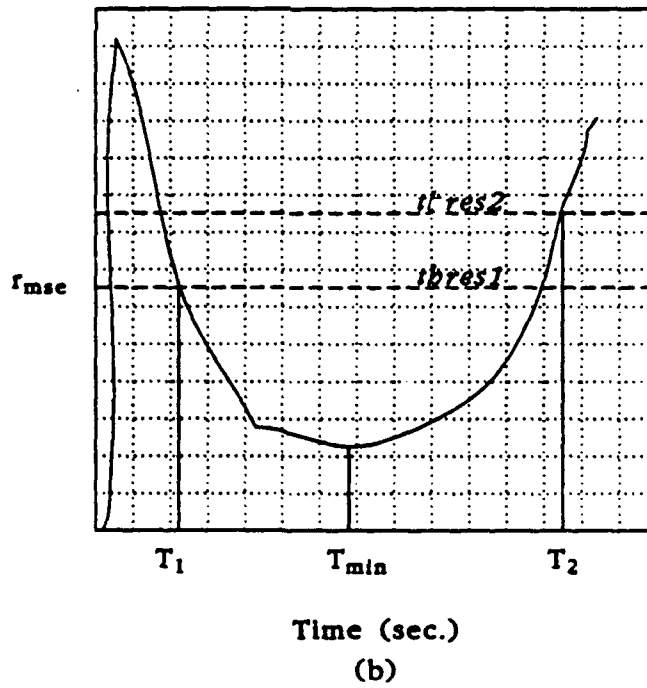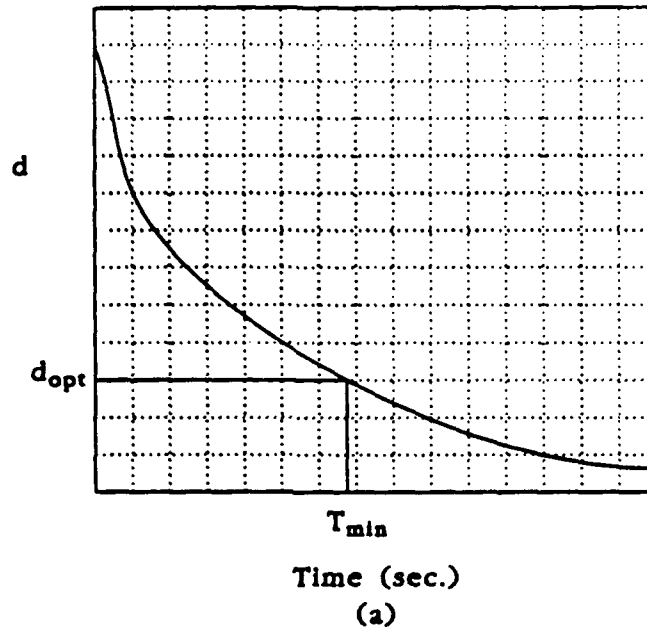
Figure 13: Illustration of the adaptive Kalman filter process.

19

where ξ_1 is a number close to 1.0. As d is decreased according to Eq. (39), a scaled version of $\overline{e_n^2}$ (scaled by an estimate of the power in u_n in Fig. 12) is monitored. This scaled term is defined as

$$r_{mse} = \overline{e_n^2}/\overline{u_n^2} \qquad (41)$$

where $\overline{u_n^2}$ is an estimate of the power, i.e.,

$$\overline{u_n^2} = \xi_2 \overline{u_{n-1}^2} + (1 - \xi_2)u_n^2 \qquad (42)$$

where ξ_2 is a number close to 1.0. Equation (42) requires a reasonable initial condition to counter the long time constants resulting from those values of ξ_2 very close to 1.0. One approach that is used in the results to follow is to produce a "quick" estimate based on the relation

$$\overline{u_j^2} = \frac{1}{j}\sum_{i=1}^{j} u_i^2 \qquad (43)$$

where j is set to some reasonable value. After j samples, Eq. (43) is replaced by Eq. (42). Another possibility is to break up the estimate of $\overline{u_n^2}$ into, say, two parts. The first part could correspond to one value of ξ_2 that would produce a quick estimate of $\overline{u_n^2}$, and the second part to another value of ξ_2 closer to 1.0, using the result from the first part as an initial condition.

An example of the type of profile created by Eq. (41) is illustrated in Fig. 13(b). The search for the minimum commences when r_{mse} first crosses the threshold defined by $thres1$ occurring at T_1 seconds. The value of d (call this d_{opt}) in Fig. 13(a) at which the minimum of r_{mse} occurs, is retained. The search ceases when r_{mse} crosses the pre-defined threshold denoted by $thres2$ at T_2 seconds. At this time d is immediately changed to the optimum value d_{opt} determined in the search phase, and the Kalman filter is re-initialized.

Two examples of the adaptive algorithm will now be discussed for two narrow-band Gaussian noise interferers of bandwidths $B_i = 0.01$ Hz and 0.05 Hz. For these examples, $E_b/N_0 = 12$ dB, the interference-to-signal ratio is 20 dB, and $L = 20$. The interference estimator was the one in Fig. 8. The low pass filter had 7 taps with rectangular weighting and was of bandwidth $B_{LPF} = 0.20$ Hz; thus the delay D was 3 samples. The phase was also smoothed over 7 samples.

A few words must be mentioned about the selection of specific values for the constants d_0 and c_0 in Eq. (39). In the examples to be considered, d_0 has been set to 1.75 rad./sec./volt, corresponding to a reasonable value obtained from Fig. 14 [3] which

---

[3]This figure shows the amount of interference suppression (i.e., $S = 10\log(\overline{\Delta i_n^2}/P_i)$ where P_i is interference power) for various values of d and interference bandwidths, B_i.

20
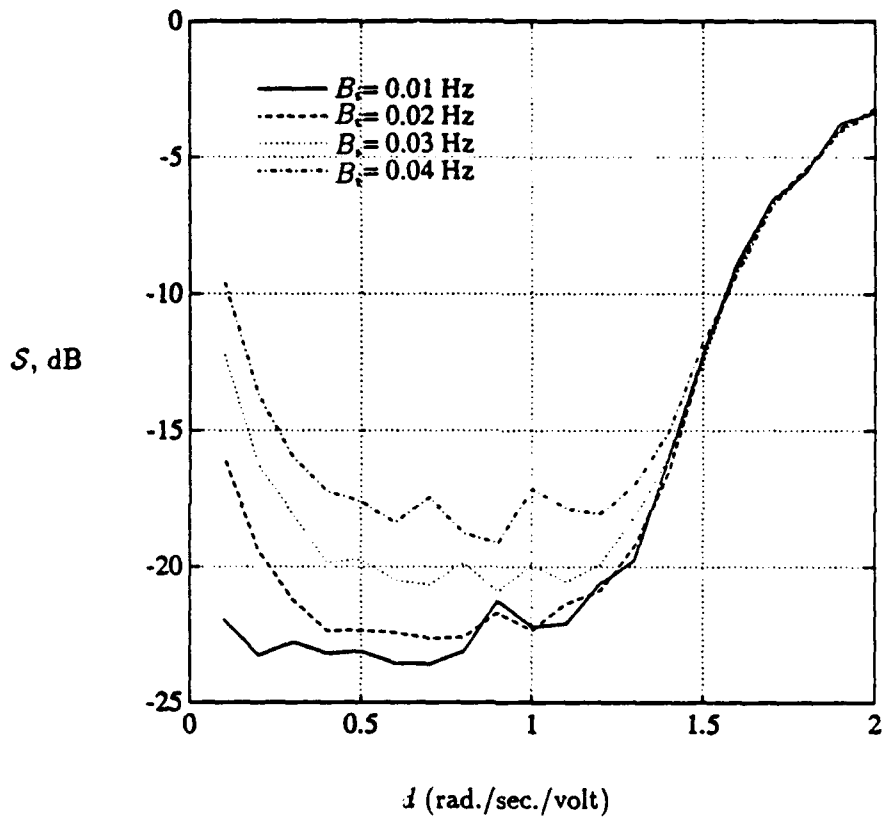
Figure 14: Interference suppression level S as a function d for several interference bandwidths, B_i, ranging from 0.01 Hz to 0.05 Hz, with $B_{LPF} = 0.20$ Hz.

21

was extracted from [12] for the interference bandwidths considered therein. The value for c_0 is selected according to the user's desired maximum change in d, i.e., Δd_{max}, over the time-constant determined by ξ_1 in Eq. (40) which estimates the power in the error signal e_n; for the examples considered, Δd_{max} was chosen to be 0.10 rad./sec./volt, and $\xi_1 = 0.999$ (a time-constant of 1000 seconds). Therefore, with $c_0 = 0.000065$ and $d_0 = 1.75$ rad./sec./volt, d was guaranteed not to change by more than 0.10 rad./sec./volt over any 1000 second interval during the search phase. This strategy provides some guidance to the user as to the rationale in selecting values for these constants, bearing in mind, however, that several trade-offs involving these parameters must be considered. These tradeoffs include the accuracy in estimating $\overline{e_n^2}$ and $\overline{u_n^2}$, speed of adaptation, the quality of the r_{mse} curve in Fig. 13(b), and the threshold levels $thres1$ and $thres2$.

Figure 15 shows the profile of the frequency deviation constant that resulted when the bandwidth of the interferer was 0.01 Hz. The steady-state value in this case was $d_{opt} = 0.30$ rad./sec./volt which agrees reasonably well with the results in Fig. 14. The error signal e_{n-D}, illustrated in Fig. 16, shows the effect of the changing deviation constant in Fig. 15. Observe that, as d becomes too small, the error signal starts to increase, indicating less interference cancellation. Towards the end, at $\approx T = 70,000$ seconds, when $thres2$ is finally crossed, the Kalman filter is re-initialized and set to a value of d_{opt}, resulting in a lower level of e_{n-D}. The mean-squared value of the reference signal u_{n-D} is illustrated in Fig. 17. The initial condition was calculated with $j = 1000$ in Eq. (43). After 1000 samples, the result $\overline{u_n^2}$ was inserted into Eq. (42) with $\xi_2 = 0.9999$

The mean-squared value of e_{n-D} was calculated using Eq. (40) with $\xi_1 = 0.999$ and scaled by $\overline{u_n^2}$ in Fig. 17. The resulting ratio r_{mse} from Eq. (41) is shown in Fig. 18. The two thresholds $thres1$ and $thres2$, were set to 0.05 (-13 dB) and 0.07 (-11.6 dB) respectively; these values were determined with the aid of Fig. 14 and experimentally. Referring to Figs. 13 and 18, $thres1$ is crossed at $T_1 \approx 4000$ seconds and $thres2$ is crossed at $T_2 \approx 71000$ seconds. The residual interference and approximate suppression level for this case are illustrated in Figs. 19 and 20. The latter figure shows an average interference suppression value of 23 dB, which agrees with the results in Fig. 14.

Figures 21 to 25 illustrate the results when the interference bandwidth has been increased to $B_i = 0.05$ Hz. As shown in Fig. 21, the final "optimum" value for d is ≈ 0.82 rad./sec./volt. This larger value for d is to be expected, since a larger bandwidth is required for the Kalman filter to track the faster varying phase. Figure 22 illustrates the power estimated in the delayed input signal u_{n-D} which, for this particular example, provided a better estimate than the one in Fig. 17; the initial condition calculated from Eq. (43) was closer to the desired value. The ratio, r_{mse}, as estimated according to

22

Eq. (41), is illustrated in Fig. 23. For this larger bandwidth interferer, the adaptive system reacts faster as compared to the case where $B_i = 0.01$ Hz, the r_{ms} of which was illustrated in Fig. 18. The residual interference, Δi_{n-D}, shown in Fig. 24, compared with the results in Fig. 19, reveals a significantly higher level of residual interference. Finally, Fig. 25 shows the average interference suppression which is approximately 17 dB after adaptation is completed.

The bit error performance of this adaptive algorithm is presented next. For this example, 10,000 bits were transmitted and the bit errors were counted over time, during and after the adaptation period. The conditions were the same as those used in the previous examples except that the interferers ranged in bandwidth from 0.01 Hz to 0.05 Hz in steps of 0.01 Hz. The bit error profiles are illustrated in Fig. 26. The profiles consist of four sections having different slopes, which correspond to the high and low levels of the residual interference results in Figs. 19 and 24. Furthermore, the times T_2 at which the adaptive algorithm switches to the optimum value for the frequency deviation constant d_{opt} occur in the pattern as expected: as B_i increases T_2 decreases.

5.0 CONCLUDING REMARKS

This report has presented an adaptive approach to interference suppression using a Kalman filter. The Kalman filter is also referred to as a digital phase-locked loop, since the system structure looks like an analog phase-locked loop. The scheme is based on varying the frequency deviation constant d of the Kalman filter over time while holding its other parameters fixed and finding that value of d which would minimize the mean-squared error at the excisor output.

The results show that this approach proves to be a valid technique. One possible drawback is the adaptation time, although the results show that significant interference rejection is achieved for much of the adaptation period. Further analysis with the various system parameters would have to be conducted in order to establish if the adaptation period could be reduced, bearing in mind, of course, that this would incur penalties in performance because of the requirement to balance several conflicting tradeoffs.

Finally, the interference which was considered in this study was narrowband Gaussian noise whose envelope and phase both vary over time. For constant envelope interference having the same bandwidth as the narrowband Gaussian noise, one would expect better performance from this type of excisor.
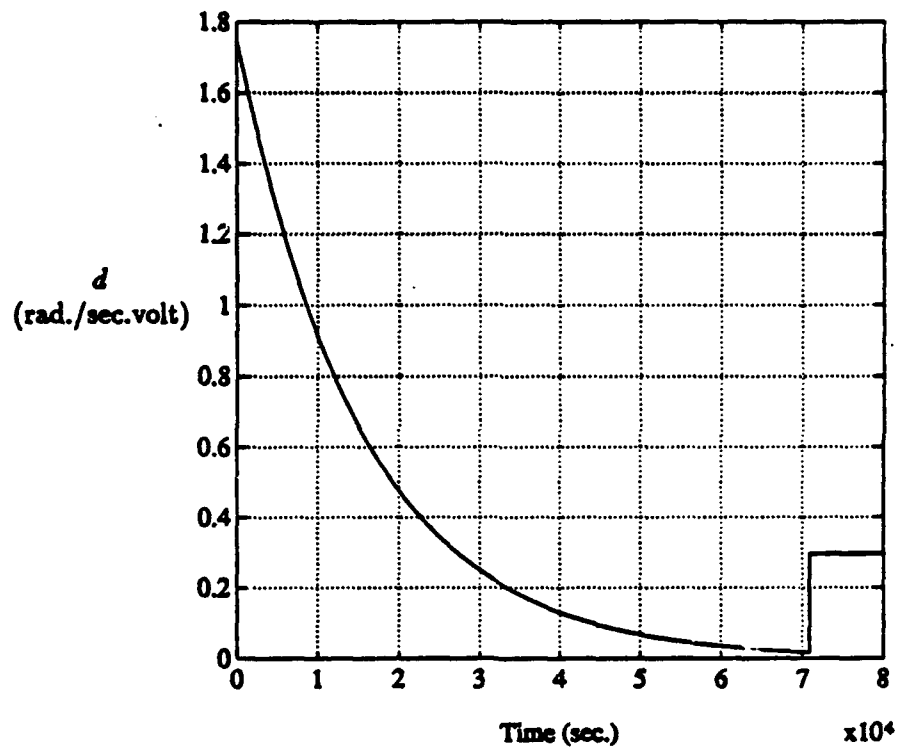
Figure 15: An example of the profile of the frequency deviation constant d used in the adaptive algorithm, $B_i = 0.01$ Hz.
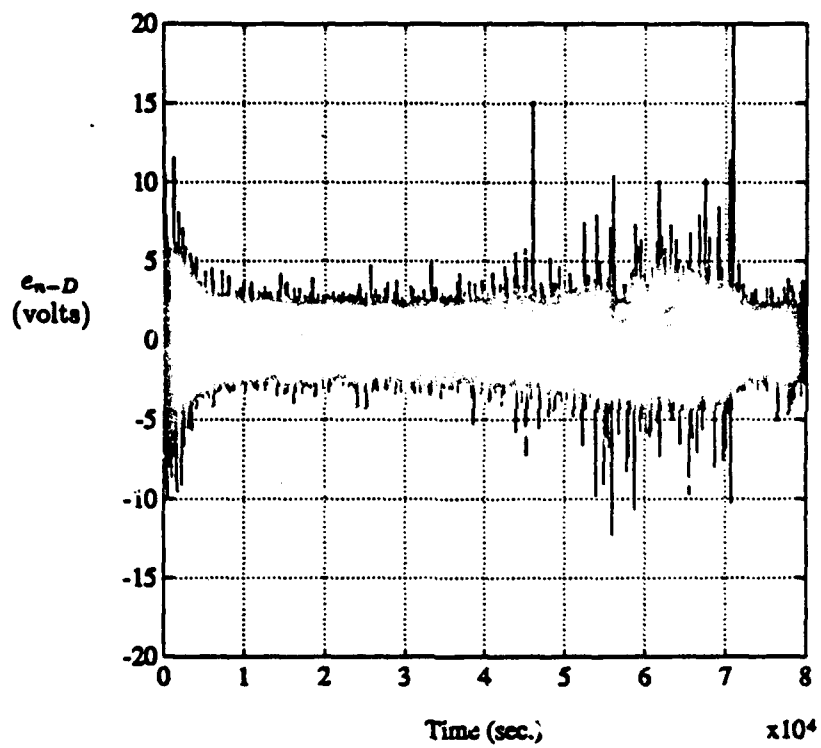
Figure 16: An example of the error signal e_{n-D} for the d profile in Fig. 15 used in the adaptive algorithm, with $B_i = 0.01$ Hz.
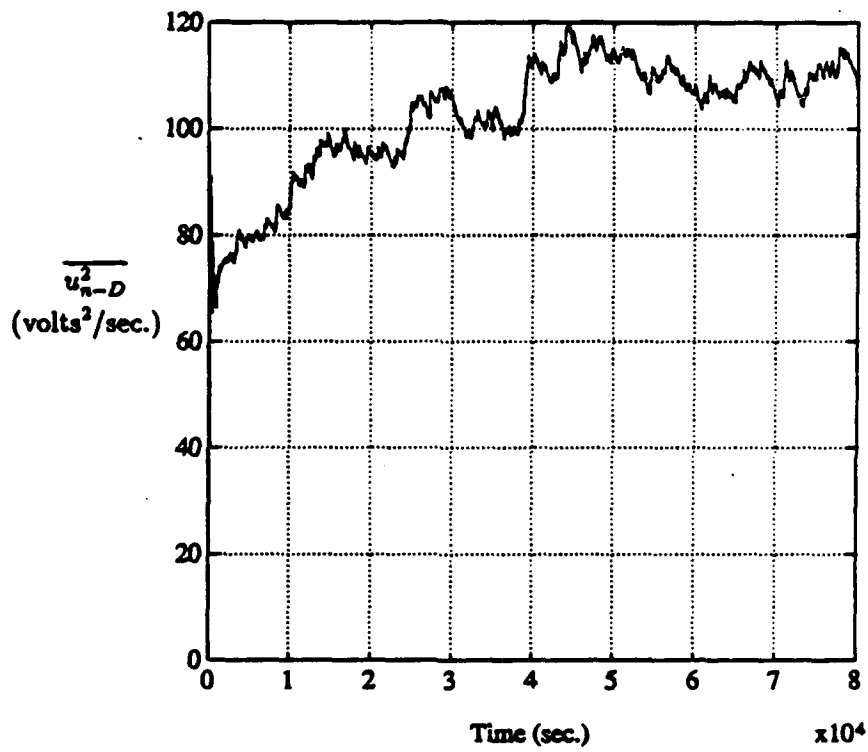
Figure 17: An example of the estimated power in u_{n-D} calculated from Eq. (42) for the d profile in Fig. 15 used in the adaptive algorithm, with $B_i = 0.01$ Hz.
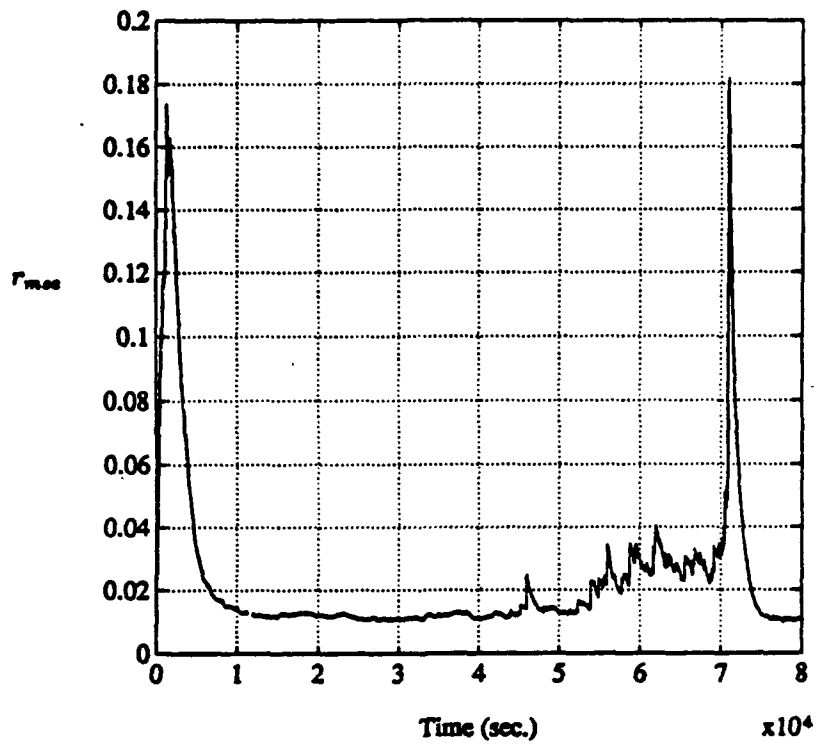
Figure 18: An example of the ratio of $r_{mse} = \overline{e_{n-D}^2}/\overline{u_{n-D}^2}$ for the d profile in Fig. 15 used in the adaptive algorithm, with $B_i = 0.01$ Hz.
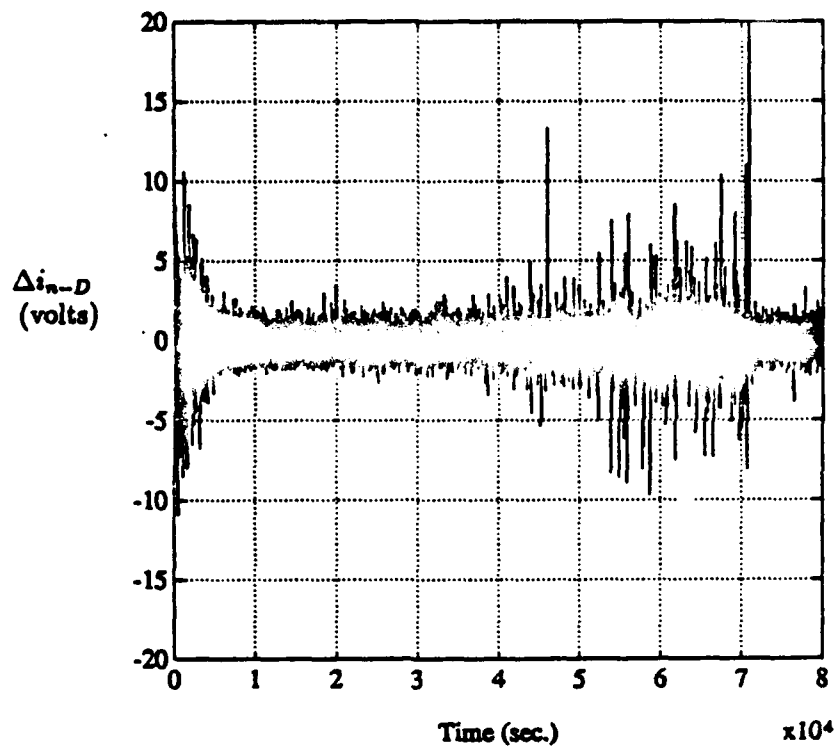
Figure 19: An example of the residual interference $\Delta i_{n-D} = i_{n-D} - \hat{i}_{n-D}$ before the despreader in the adaptive algorithm, with $B_i = 0.01$ Hz.
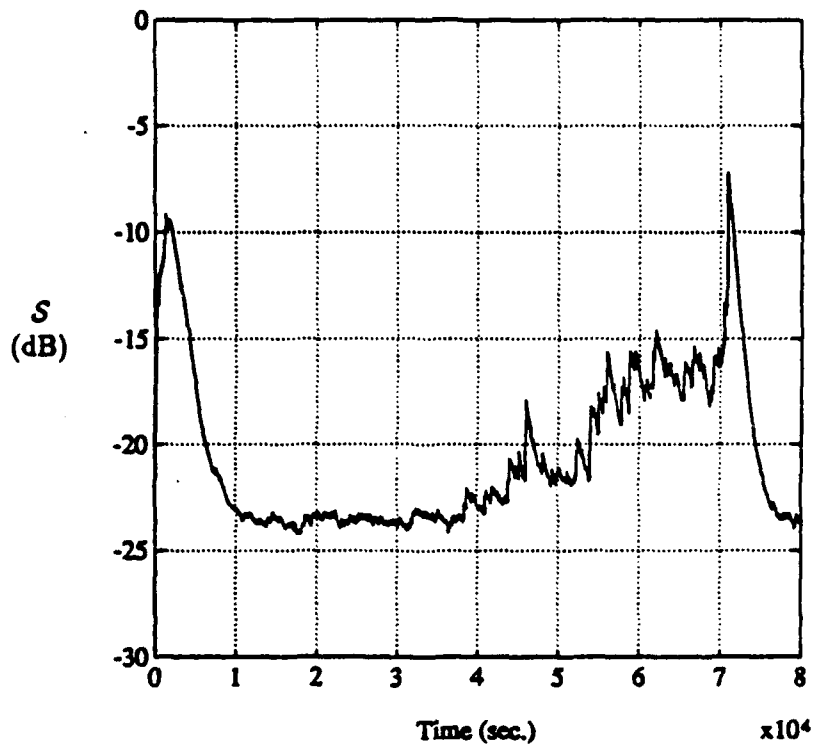
Figure 20: An example illustrating the degree of interference suppression $10 \log(\overline{\Delta i_{n-D}^2}/P_i)$, where $P_i = 100$ is the power in the interferer of bandwidth $B_i = 0.01$ Hz.
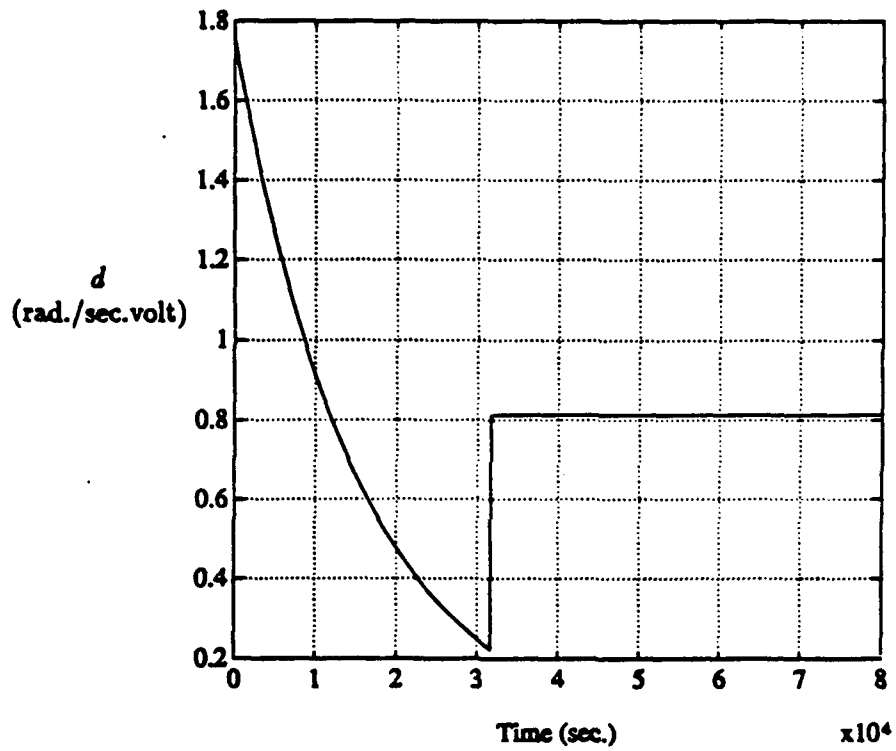
Figure 21: An example of the profile of the frequency deviation constant d used in the adaptive algorithm, $B_i = 0.05$ Hz.
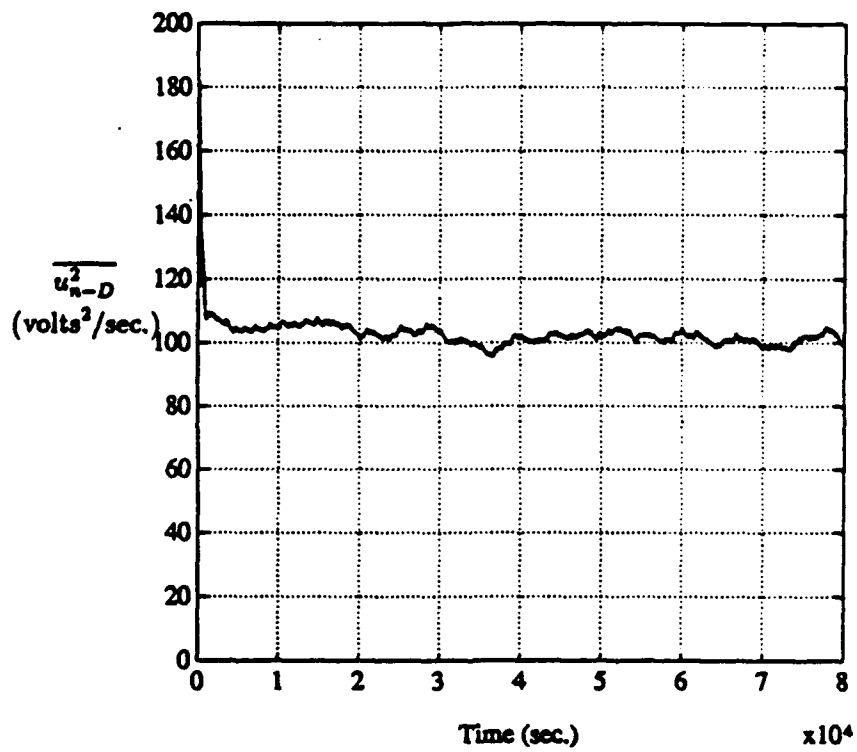
Figure 22: An example of the estimated power in u_{n-D} calculated from Eq. (42) for the d profile in Fig. 21 used in the adaptive algorithm, with $B_i = 0.05$ Hz.
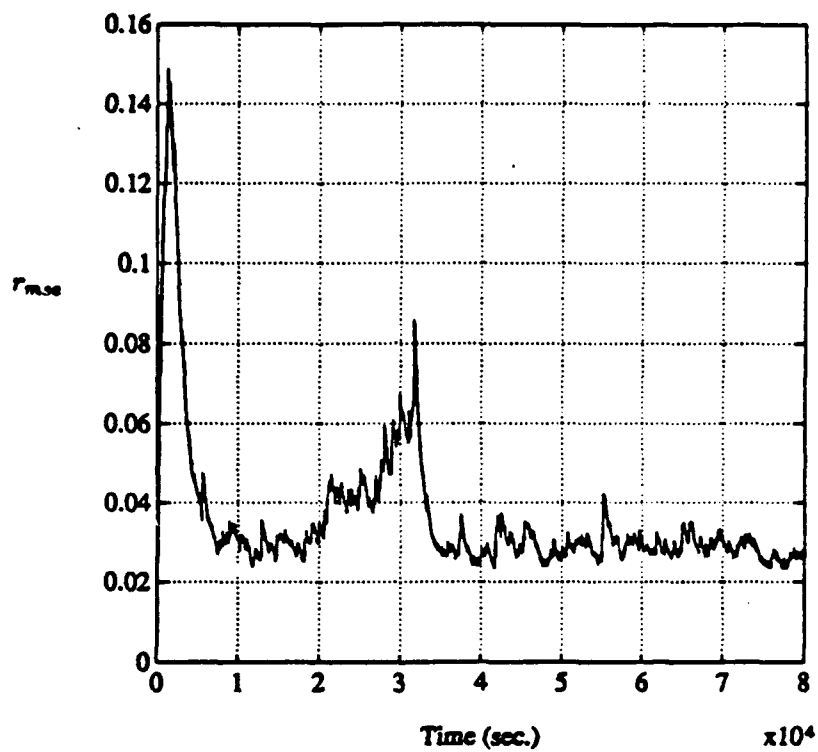
Figure 23: An example of the ratio of $r_{mse} = \overline{e_{n-D}^2}/\overline{u_{n-D}^2}$ for the d profile in Fig. 21 used in the adaptive algorithm, with $B_t = 0.05$ Hz.

32
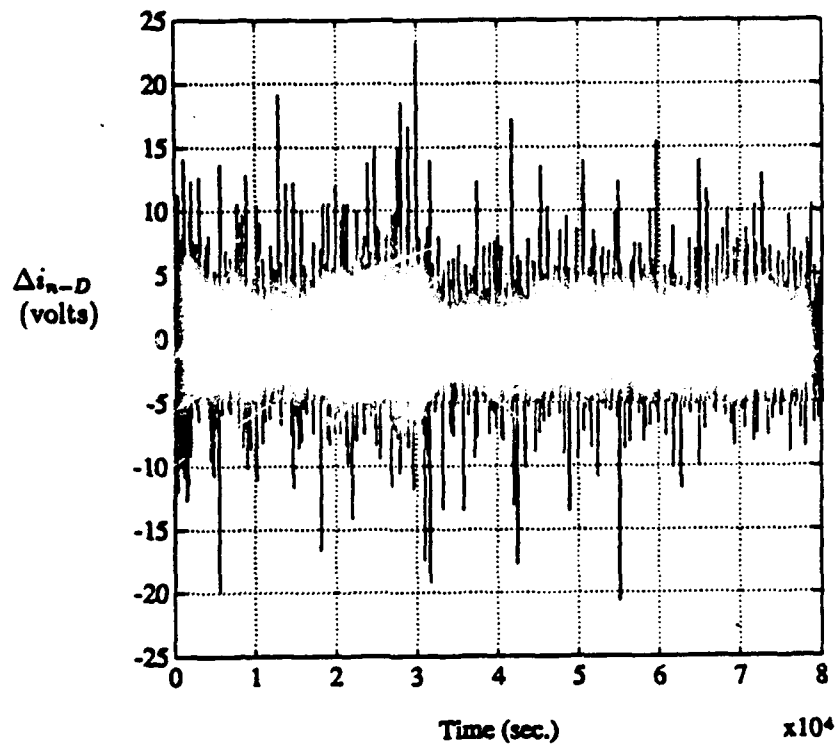
Figure 24: An example of the residual interference $\Delta i_{n-D} = i_{n-D} - \hat{i}_{n-D}$ before the despreader in the adaptive algorithm, with $B_i = 0.05$ Hz.
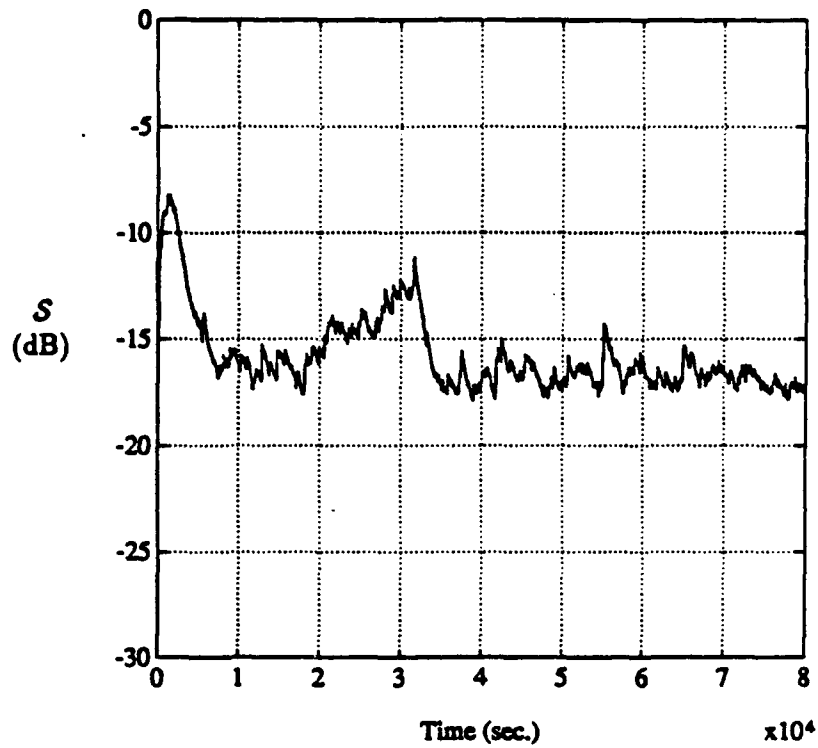
Figure 25: An example illustrating the degree of interference suppression $10\log(\overline{\Delta i^2_{n-D}}/P_i)$, where $P_i = 100$ is the power in the interferer of bandwidth $B_i = 0.05$ Hz.

34
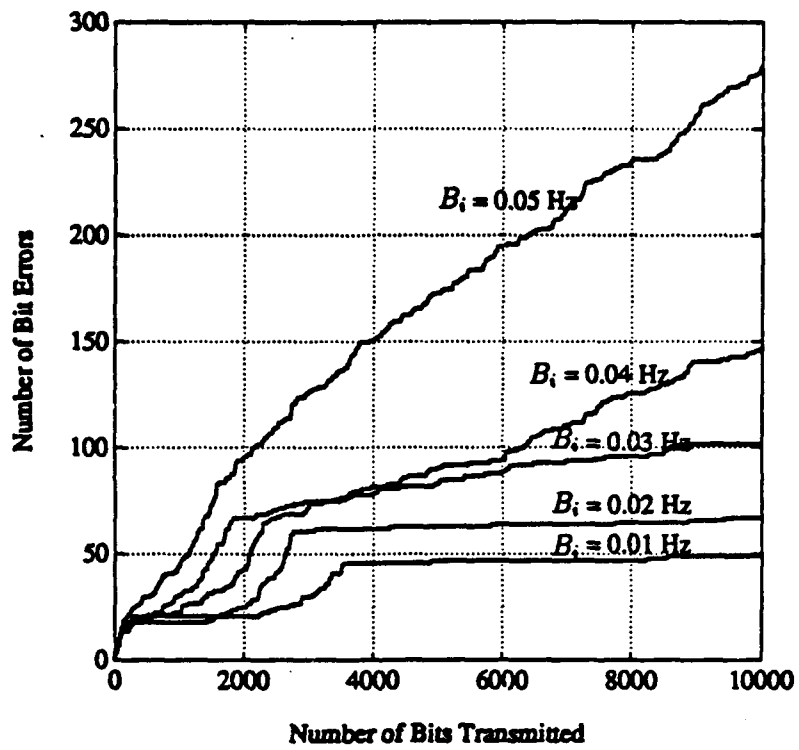
Figure 26: Bit error performance of the adaptive scheme for several interference bandwidths and $E_b/N_0 = 12$ dB using the interference estimator in Fig. 8.

REFERENCES

[1] B. W. Kozminchuk and A. U. H. Sheikh, "A Kalman filtering technique for suppressing jammers in direct sequence spread spectrum communication systems," in *Queens 50th Biennial Symposium on Communications*, pp. 5-8, June 1990. Kingston, Ontario.

[2] B. W. Koz·· nchuk, "Excision techniques in direct sequence spread spectrum communication systems," Technical Report 1047, Defence Research Establishment Ottawa, Ottawa, Ontario, Canada, K1A 0Z4, 1990.

[3] B. W. Kozminchuk, "Kalman filter-based architectures for interference excision," Technical Report 1118, Defence Research Establishment Ottawa, Ottawa, Ontario, Canada, K1A 0Z4, 1991.

[4] B. W. Kozminchuk, "A comparison of recursive least squares and Kalman filtering excisors for swept tone interference," Technical Note 92-14, Defence Research Establishment Ottawa, Ottawa, Ontario, Canada, K1A 0Z4, 1992.

[5] B. W. Kozminchuk, "Theoretical bit error rate performance of the Kalman filter excisor for FM interference," Technical Report 1163, Defence Research Establishment Ottawa, Ottawa, Ontario, Canada, K1A 0Z4, 1993.

[6] A. Blanchard, *Phase-Locked Loops*. New York: John Wiley and Sons, 1976.

[7] D. R. Polk and S. C. Gupta, "Quasi–optimum digital phase–locked loops," *IEEE Transactions on Communications*, vol. 21, pp. 75–82, January 1973.

[8] A. P. Sage and J. L. Melsa, *Estimation Theory with Applications to Communications and Control.* New York: McGraw-Hill, 1971.

[9] H. L. Van Trees, *Detection, Estimation, and Modulation–Part 2: Nonlinear Modulation Theory.* New York: John Wiley and Sons, 1971.

[10] C. N. Kelly and S. C. Gupta, "The digital phase-locked loop as a near-optimum FM demodulator," *IEEE Transactions on Communications*, vol. 20, pp. 406–411, June 1972.

[11] D. F. Liang, "Comparisons of nonlinear recursive filters for systems with non-negligible nonlinearities," in *Control and Dynamic Systems: Advances in Theory and Applications- Volume 20* (C. T. Leondes, ed.), Academic Press, 1983.

REF-1

REFERENCES

[12] B. W. Kozminchuk, "An improved Kalman filter excisor for suppressing narrowband Gaussian noise interference," Technical Note 92-28, Defence Research Establishment Ottawa, Ottawa, Ontario, Canada, K1A 0Z4, 1992.

DOCUMENT CONTROL DATA

(Security classification of title, body of abstract and indexing annotation must be entered when the overall document is classified)

1. ORIGINATOR (the name and address of the organization preparing the document. Organizations for whom the document was prepared, e.g. Establishment sponsoring a contractor's report, or tasking agency, are entered in section 8.)	2. SECURITY CLASSIFICATION (overall security classification of the document. including special warning terms if applicable)
DEFENCE RESERCH ESTABLISHMENT OTTAWA NATIONAL DEFENCE SHIRLEY BAY, OTTAWA, ONTARIO K1A 0K2 CANADA	UNCLASSIFIED

3. TITLE (the complete document title as indicated on the title page. Its classification should be indicated by the appropriate abbreviation (S,C or U) in parentheses after the title.)

AN ADAPTIVE KALMAN FILTER EXCISOR FOR SUPPRESSING NARROWBAND INTERFERENCE (U)

4. AUTHORS (Last name, first name, middle initial)

KOZMINCHUK, BRIAN W.

5. DATE OF PUBLICATION (month and year of publication of document) NOVEMBER 1993	6a. NO. OF PAGES (total containing information. Include Annexes, Appendices, etc.) 45	6b. NO. OF REFS (total cited in document) 12

7. DESCRIPTIVE NOTES (the category of the document, e.g. technical report, technical note or memorandum. If appropriate, enter the type of report, e.g. interim, progress, summary, annual or final. Give the inclusive dates when a specific reporting period is covered.)

DREO TECHNICAL NOTE 93-20

8. SPONSORING ACTIVITY (the name of the department project office or laboratory sponsoring the research and development. Include the address.)

DEFENCE RESEARCH ESTABLISHMENT OTTAWA
NATIONAL DEFENCE
SHIRLEY BAY, OTTAWA, ONTARIO K1A 0K2 CANADA

9a. PROJECT OR GRANT NO. (if appropriate, the applicable research and development project or grant number under which the document was written. Please specify whether project or grant) 041LK11	9b. CONTRACT NO. (if appropriate, the applicable number under which the document was written)
10a. ORIGINATOR'S DOCUMENT NUMBER (the official document number by which the document is identified by the originating activity. This number must be unique to this document.)	10b. OTHER DOCUMENT NOS. (Any other numbers which may be assigned this document either by the originator or by the sponsor)

11. DOCUMENT AVAILABILITY (any limitations on further dissemination of the document, other than those imposed by security classification)

(XX) Unlimited distribution
( ) Distribution limited to defence departments and defence contractors; further distribution only as approved
( ) Distribution limited to defence departments and Canadian defence contractors; further distribution only as approved
( ) Distribution limited to government departments and agencies; further distribution only as approved
( ) Distribution limited to defence departments; further distribution only as approved
( ) Other (please specify):

12. DOCUMENT ANNOUNCEMENT (any limitation to the bibliographic announcement of this document. This will normally correspond to the Document Availability (11). However, where further distribution (beyond the audience specified in 11) is possible, a wider announcement audience may be selected.)

DCD03 2/06/87

13. ABSTRACT (a brief and factual summary of the document. It may also appear elsewhere in the body of the document itself. It is highly desirable that the abstract of classified documents be unclassified. Each paragraph of the abstract shall begin with an indication of the security classification of the information in the paragraph (unless the document itself is unclassified) represented as (S), (C), or (U). It is not necessary to include here abstracts in both offical languages unless the text is bilingual.)

(U)   Several reports have been written by the author which characterize the performance of a Kalman filtering technique to suppress narrowband interference from direct sequence spread spectrum communications systems in a non-adaptive context, i.e., when the user has some a priori knowledge of the interference characteristics. This report expands on this technique by presenting an adaptive scheme which is useful for the situation when the interference characteristics are unknown. In this context, the Kalman filter must "learn" to achieve optimal performance through the adjustment of one of its parameters. The criterion for optimality is the minimization of the mean-squared error at the output of the canceller, where this error consists of spread spectrum signal, noise and residual interference. The reasonable assumption is made that minimizing the mean of this squared error with respect to the appropriate Kalman filter parameter is equivalent to minimizing the mean squared value of the residual interference. Examples of the dynamic behaviour of the adaptive interference suppressor are presented for narrowband Gaussian noise interference with bandwidths ranging from 1 to 5% of the chip rate.

14. KEYWORDS, DESCRIPTORS or IDENTIFIERS (technically meaningful terms or short phrases that characterize a document and could be helpful in cataloguing the document. They should be selected so that no security classification is required. Identifiers, such as equipment model designation, trade name, military project code name, geographic location may also be included. If possible keywords should be selected from a published thesaurus, e.g. Thesaurus of Engineering and Scientific Terms (TEST) and that thesaurus-identified. If it is not possible to select indexing terms which are Unclassified, the classification of each should be indicated as with the title.)

SPREAD SPECTRUM
KALMAN FILTER
PHASE-LOCKED LOOP
INTERFERENCE SUPPRESSION
EXCISION
·OPTIMUM FILTER